Interbeat interval variability versus frequency modulation of heart rate

M. D. Prokhorov [1,*] A. S. Karavaev,[1,2,3] Y. M. Ishbulatov,[1,2,3] V. I. Ponomarenko [1,2] A. R. Kiselev,[2,3] and J. Kurths[2,4,5]

[1]*Saratov Branch of Kotelnikov Institute of Radio Engineering and Electronics of Russian Academy of Sciences,*
Zelyonaya Street 38, Saratov 410019, Russia
[2]*Saratov State University, Astrakhanskaya Street 83, Saratov 410012, Russia*
[3]*Institute of Cardiological Research, Saratov State Medical University, Saratov, B. Kazachaya Street, 112, Saratov 410012, Russia*
[4]*Physics Department, Humboldt University, Newtonstrasse 15, 12489 Berlin, Germany*
[5]*Potsdam Institute for Climate Impact Research, Telegrafenberg A31, 14473 Potsdam, Germany*

The heart rate in humans is regulated by the autonomic nervous system, which modulates the frequency of heart contractions, resulting in heart rate variability (HRV). Therefore, to assess the activity of the autonomic nervous system, which contains important information for medical diagnostics, methods based on the analysis of interbeat interval variability are often used. This approach does not require the use of invasive methods for measuring the signals of the autonomic nervous system, but its accuracy is an open question. Using mathematical modeling, we investigate the possibility of extracting the signal of frequency modulation of the heartbeats from the electrocardiogram (ECG) signal and conduct a detailed comparison of the extracted signal with the real modulating signal. Since the quality of extraction of the signal of frequency modulation from the ECG depends on the method of demodulation, we compare two different approaches. One is based on the detection of the main oscillation rhythm and its bandpass filtering, and the other on the heterodyning technique. It is shown that low-frequency (LF) and high-frequency (HF) oscillations in HRV associated, respectively, with sympathetic and parasympathetic modulation by the autonomic nervous system, in the general case, significantly differ from the signals of frequency modulation of the heart rate in shape, but have close similarity with them in the frequency domain. We find that in model systems, the similarity of the LF component of HRV with sympathetic modulation of the heart rate is higher than the similarity of the HF component of HRV with parasympathetic modulation.

I. INTRODUCTION

The heart is a nonlinear nonautonomous self-oscillating system. Its electrical activity is spontaneously generated by the sinoatrial node, which sets the rhythm of the heart (about 60–90 beats per minute) and so is known as the heart's natural pacemaker [1]. However, the heart rate is not constant. It is modulated by the autonomic nervous system that innervates the sinoatrial node via both sympathetic and parasympathetic tracts [2]. Such a modulation provides a quick and flexible adaptation of a healthy heart to changes in the level of physical and emotional activity and environmental influences. The regulation of the heart rate by the autonomic nervous system leads to the appearance of heart rate variability (HRV), which is understood as a variation of interbeat intervals [3]. Since interbeat intervals are usually defined as the intervals between the well-pronounced R peaks in an electrocardiogram (ECG), they are often called RR intervals.

Spectral analysis of HRV allows one to study effects of frequency modulation of the sinoatrial node by the nervous system. In the power spectrum of RR intervals, low-frequency (LF) and high-frequency (HF) components are distinguished. The power and central frequency of these components may vary in relation to changes in autonomic modulations of the heart rate [4]. It is generally accepted that in the power spectrum of RR intervals, the frequency range 0.04–0.15 Hz refers to the LF component and the frequency range 0.15–0.4 Hz to the HF component of HRV [3].

The main contribution to the HF component of HRV is made by respiratory oscillations that modulate the heart rate. The heart rate increases during inspiration and decreases during expiration, resulting in respiratory sinus arrhythmia (RSA) [5]. The intensity of RSA can be used to assess the vagal activity [6], whose value is important for the diagnostics of certain diseases. For example, RSA analysis is used in psychiatry to assess mental health [7–9]. Moreover, RSA is usually reduced in heart failure, myocardial infarction, and stroke.

Various methods have been proposed for a quantitative assessment of RSA [10,11]. Respiratory-associated oscillations in HRV can be extracted using the decomposition of the spectrum [12], bandpass filtering [13], empirical mode decomposition [14,15], or wavelet analysis [16]. In Refs. [17,18], a method was proposed for extracting the respiratory-related component of HRV using the reconstruction of the phase dynamics of the cardiac and respiratory systems from simultaneous measurements of ECG and respiratory flow.

The origin of LF oscillations in HRV is still a subject of controversy [19,20]. It is believed that LF oscillations in

---

*mdprokhorov@yandex.ru

heart rate are a marker of sympathetic modulation by the autonomic nervous system [21–23]. However, a number of authors assume that arterial baroreceptors are also involved in the generation of LF oscillations [24–26]. Since sympathetic activity is well established to be elevated in heart failure [27] and coronary artery disease [28] and may be associated with the initiation of hypertension [29,30], a quantitative assessment of autonomic tone is of great importance for medical diagnostics.

LF variation of heart rate is associated with Mayer waves of blood pressure and usually has a frequency of about 0.1 Hz [25,26,31,32]. The index of synchronization between 0.1-Hz oscillations in the heart rate and blood pressure is an important factor for diagnostics of the functional state of the cardiovascular system [33–35]. It is used in cardiac surgery [36], gynecology [37], and personalized therapy of patients after myocardial infarction [38]. To extract the LF component of HRV, one can use the above-mentioned methods [12–16], employed for extracting the HF component of HRV.

Thus, acting on the sinoatrial node, the autonomic nervous system carries out frequency modulation of the heart rate in the LF and HF ranges. Modulating signals reflecting sympathetic activity and parasympathetic (vagal) activity contain important information, both for studying the physiology of the cardiovascular system and for medical diagnostics. However, a direct measurement of signals from the autonomic nervous system requires the use of invasive methods [39–41] that limits their application. Therefore, to obtain information about the activity of the autonomic nervous system, methods based on the analysis of ECG and RR intervals are widely used. This brings up the following legitimate question: How accurate is this approach and what are its limitations [42]?

In this paper, we investigate the possibility of extracting the signal of frequency modulation from the ECG signal and conduct a detailed comparison of the extracted signal with the real modulating signal. This allows us to understand how accurately the interbeat interval variability reflects the frequency modulation of the heart rate by the autonomic nervous system. Since the possibilities of carrying out a detailed physiological experiment involving invasive signal measurements are very limited, we present here a study on mathematical modeling. Three types of frequency modulation of the basic rhythm of the model system are considered: harmonic, two-frequency, and broadband. Two approaches are used to extract the signal of frequency modulation. The first approach is based on the detection of the main oscillation rhythm and its bandpass filtering. The second approach is based on the heterodyning technique, which is widely used in radio receivers and communication systems [43]. Note that both of these approaches use only a frequency-modulated signal for the analysis and, in contrast to the method [18], do not require a record of the modulating signal.

The paper is organized as follows. In Sec. II, we describe the mathematical models used to study how accurately the interbeat interval variability reflects the frequency modulation of the heart rate. Section III contains the description of methods of demodulation. In Sec. IV, we compare the time series and power spectra of modulating signals with the time series and power spectra of signals extracted from the frequency-modulated signals of model oscillators. The results are summarized in Sec. V.

II. MODEL SYSTEMS

The isolated human heart contracts due to the self-oscillating activity of the sinoatrial node and generates almost periodic oscillations. In the human body, the regulation of the heart rate is carried out by the autonomic nervous system, which adjusts the frequency of heartbeats to the needs of the organism. To illustrate the process of frequency modulation of self-oscillations, let us first consider the simplest case, when an autonomous oscillator generates a harmonic signal

$$u(t) = A \cos{(2\pi f_h t)}, \tag{1}$$

where A and f_h are the amplitude and frequency of oscillations, respectively. If f_h is modulated with the signal $m(t)$, then the frequency-modulated signal can be written as follows:

$$h(t) = A \cos{\left(2\pi f_h t + 2\pi f_\Delta \int_0^t m(\tau)d\tau\right)}, \tag{2}$$

where f_Δ is the frequency deviation. In the simplest case, the modulating signal is harmonic:

$$m(t) = \cos{(2\pi f_m t)}, \tag{3}$$

where f_m is the frequency of modulation. In this case, Eq. (2) takes the form

$$h(t) = A \cos{[2\pi f_h t + B \sin{(2\pi f_m t)}]}, \tag{4}$$

where $B = f_\Delta / f_m$ is the modulation index.

Using the expansion of the signal $h(t)$ in the Fourier series, Eq. (4) can be rewritten as

$$h(t) = A \sum_{k=-\infty}^{\infty} J_k(B) \cos{[2\pi(f_h + kf_m)t]}, \tag{5}$$

where $J_k(B)$ is the Bessel function and $k \in \mathbf{Z}$ is the order of the Bessel function. From Eq. (5) it follows that the power spectrum of $h(t)$ contains an infinite number of sidebands that are symmetric with respect to f_h and their power decreases with increasing $|k|$.

Figure 1 schematically illustrates the case of frequency modulation of a harmonic signal $u(t)$ having the frequency $f_h = 1$ Hz by a harmonic modulating signal $m(t)$ with $f_m = 0.1$ Hz. As a result, we obtain a frequency-modulated signal $h(t)$, whose power spectrum S_h has a main peak at f_h and peaks at the frequencies $f_h \pm nf_m$, where n is a positive integer.

Of course, the self-oscillations of the real sinoatrial node are not harmonic as well as the signals of the autonomic nervous system that modulate them. Therefore, the frequency-modulated signal of the heart activity will have a more complicated spectrum than the signal (5). Real physiological signals are very complex and it is not possible to obtain strict analytical expressions for their spectra.

We used two mathematical models to study the possibility of extracting the signal of frequency modulation from a frequency-modulated signal. As the first paradigmatic model,
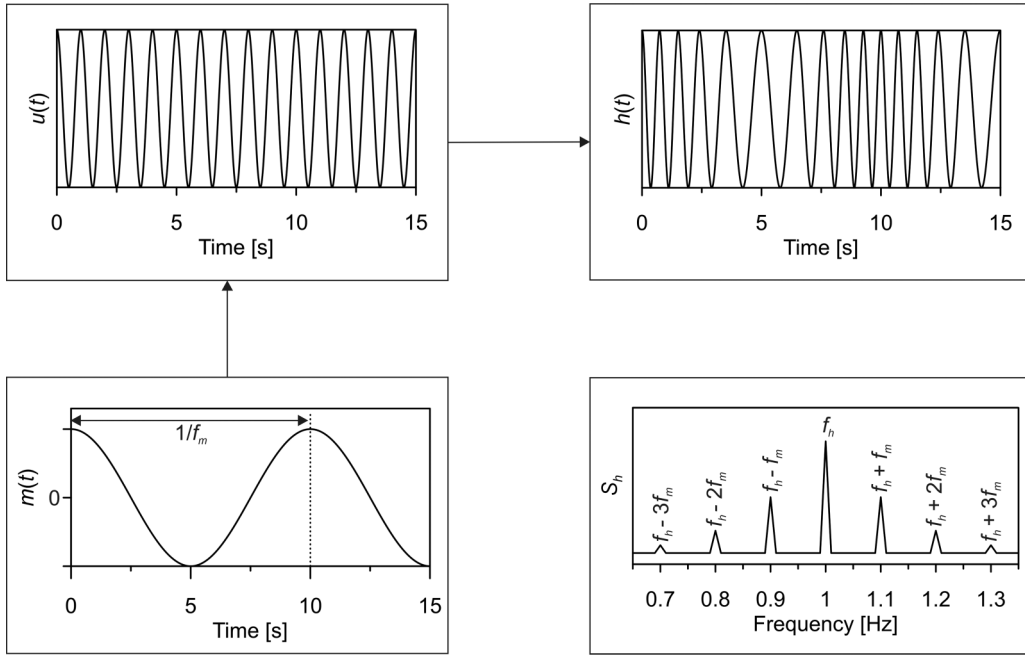
FIG. 1. Scheme of the simplest case of frequency modulation. $u(t)$ is a harmonic signal with the frequency $f_h = 1$ Hz, $m(t)$ is a harmonic modulating signal with the frequency $f_m = 0.1$ Hz, $h(t)$ is a frequency-modulated signal, and S_h its power spectrum.

we chose the frequency-modulated Van der Pol oscillator:

$$\ddot{h}(t) - \mu\left[1 - h^2(t)\right]\dot{h}(t) + \{2\pi[f_h + m(t)]\}^2 h(t) = 0, \quad (6)$$

where μ is the parameter of nonlinearity. Note that for uniformity, we used the same notation for the dynamical variable $h(t)$ and the modulating signal $m(t)$ as in Eqs. (2) and (3), respectively. The base frequency of the oscillator was set to $f_h = 1$ Hz, and $\mu = 0.2$. The Van der Pol oscillator was chosen because it is a standard nonlinear oscillator that demonstrates periodic self-sustained oscillations, the frequency of which can be matched to the frequency f_h of the main heart rhythm. Moreover, it is rather easy to understand and explain the results obtained for this oscillator.

Equation (6) was integrated numerically using a fourth-order Runge-Kutta method with a fixed time step $\Delta t = 0.004$ s. This integration step corresponds to the typical sampling time of experimental ECG signals.

As the second model, we chose a mathematical model [44], which is capable of generating realistic synthetic ECG signals, and added a modulating signal $m(t)$ into it. The model is described by the following equations:

$$\begin{aligned}
\dot{x}(t) &= \left(1 - \sqrt{x^2(t) + y^2(t)}\right)x(t) - 2\pi[f_h + m(t)]y(t), \\
\dot{y}(t) &= \left(1 - \sqrt{x^2(t) + y^2(t)}\right)y(t) - 2\pi[f_h + m(t)]x(t), \\
\dot{h}(t) &= \sum_{j=1}^{5} a_j F(\theta_j, b_j) - h(t),
\end{aligned} \quad (7)$$

where the function F is

$$F(\theta_j, b_j) = -z \exp\left(-\frac{z^2}{2b_j^2}\right) \quad (8)$$

with

$$z = \left[\arctan\left(\frac{y}{x}\right) - \theta_j\right] \mod 2\pi. \quad (9)$$

The values of the function (8) are close to zero most of the time, and only at the moments of time corresponding to P, Q, R, S, and T peaks and troughs of the ECG wave form, they increase in absolute value, providing impulse disturbance of the trajectory [44]. We used the same set of parameters as in Ref. [44]: $a_1 = 1.2$, $b_1 = 0.25$, $\theta_1 = -\pi/3$, $a_2 = -5$, $b_2 = 0.1$, $\theta_2 = -\pi/12$, $a_3 = 30$, $b_3 = 0.1$, $\theta_3 = 0$, $a_4 = -7.5$, $b_4 = 0.1$, $\theta_4 = \pi/12$, $a_5 = 0.75$, $b_5 = 0.4$, and $\theta_5 = \pi/2$. The base frequency of self-oscillations was set to $f_h = 1$ Hz. Equations (7) were integrated numerically using a fourth-order Runge-Kutta method also with a fixed time step $\Delta t = 0.004$ s.

We considered three types of modulating signals $m(t)$ in Eqs. (6) and (7) with increasing complexity. The first and simplest case is the harmonic form of $m(t)$. There, $m(t)$ is described by Eq. (3). We considered two characteristic frequencies of modulation, $f_m = 0.1$ Hz and $f_m = 0.29$ Hz. The first of them simulates the sympathetic modulation of the heart rate by the autonomic nervous system, and the second one simulates the parasympathetic modulation.

The second of the considered signals $m(t)$ corresponds to the two-frequency modulation:

$$m(t) = A_1 \cos\left(2\pi f_{m1}t\right) + A_2 \cos\left(2\pi f_{m2}t\right), \quad (10)$$

where $A_1 = 1$, $f_{m1} = 0.1$ Hz, $A_2 = 0.16$, and $f_{m2} = 0.29$ Hz. In model studies, the frequency f_{m2} corresponding to the frequency of respiration is often set to 0.25 or 0.3 Hz. We chose $f_{m2} = 0.29$ Hz to avoid a simple multiple frequency ratio $n_1 f_{m1} = n_2 f_{m2}$, where n_1 and n_2 are positive integers. The ratio of amplitudes A_1/A_2 was chosen in such a way as to provide the LF/HF ratio of HRV components typical for the spectrum of observed RR intervals of a healthy subject.

Real signals of the autonomic nervous system that regulate the heart rate are broadband and noisy. As the third type of

frequency modulation, we therefore consider the modulation of f_h by a broadband signal $m(t)$, whose spectrum is similar to that of experimental sequences of RR intervals and is described by the equation

$$S(f) = \frac{\sigma_1^2}{\sqrt{2\pi c_1^2}} \exp\left(-\frac{(f-f_1)^2}{2c_1^2}\right) + \frac{\sigma_2^2}{\sqrt{2\pi c_2^2}}$$

$$\times \exp\left(-\frac{(f-f_2)^2}{2c_2^2}\right) + \frac{c_3}{f+f_3}, \tag{11}$$

where $f_1 = 0.1$ Hz, $f_2 = 0.29$ Hz, $f_3 = 1$ Hz, $c_1 = c_2 = c_3 = 0.022$, $\sigma_1 = 0.225$, and $\sigma_2 = 0.135$. The time series and power spectrum of the broadband modulating signal $m(t)$ are shown in Sec. IV.

Figure 2 shows the time series and power spectra of the frequency-modulated Van der Pol oscillator (6) and the model of ECG signal (7). Figures 2(a) and 2(b) correspond to the case of harmonic modulation of the oscillator frequency f_h by the signal (3) with $f_m = 0.1$ Hz. As seen in Fig. 2(a), the characteristic period of oscillations of both oscillators varies in time. The power spectra in Fig. 2(b) have the main peak at $f_h = 1$ Hz and peaks at the frequencies $f_h \pm n f_m$, where n is a positive integer. In the power spectrum of the model of ECG signal, there are also peaks at the frequencies $n f_m$ and $2 f_h - n f_m$, Fig. 2(b). Figures 2(c) and 2(d) correspond to the case of harmonic modulation of f_h by the signal (3) with $f_m = 0.29$ Hz. They have the same features as Figs. 2(a) and 2(b). Figures 2(e) and 2(f) show the case of two-frequency modulation of f_h by the signal (10) with $f_{m1} = 0.1$ Hz and $f_{m2} = 0.29$ Hz. The power spectra of $h(t)$ are rather complex and have peaks at the frequencies f_h, $f_h \pm n f_{m1}$, and $f_h \pm n f_{m2}$, Fig. 2(f). The case of modulation of f_h by a broadband signal, whose spectrum is described by Eq. (11), is shown in Figs. 2(g) and 2(h). In the power spectra, the peak at the frequency f_h is most pronounced, Fig. 2(h).

III. METHODS

We compare two methods of extracting the modulating signal $m(t)$ from the signal $h(t)$ of a frequency-modulated oscillator. The first method is the most common in the study of HRV and is as follows. First, the main oscillation rhythm is detected in the signal $h(t)$. In the case of an ECG signal, the R peak is usually detected as the most pronounced [3]. For other signals, it is possible to determine, for example, the moment in time when the trajectory crosses a certain section plane, which is chosen in such a way that its crossing occurs once during a characteristic period of oscillations. Then the duration of time intervals between two successive R peaks (crossings of the section plane) is determined and a sequence of RR intervals (characteristic periods of oscillations) is obtained. The points of this sequence are not equidistant in time. To obtain an equidistant time series, the sequence is interpolated and the points are sampled with a constant sampling frequency for further analysis [14]. To extract the LF and HF components of HRV, the above-mentioned methods [12–18] are often applied. In the present paper, we use bandpass filtering in the 0.04–0.4-Hz band. This method of extracting the signal $m(t)$, based on the analysis of the characteristic periods of oscilla-

tions, we will call for brevity the ACP method (abbreviation for the analysis of characteristic periods). We denoted the modulating signal extracted via ACP as $\hat{m}(t)$.

It should be emphasized that when analyzing experimental ECG signals, the ACP method is equivalent to the standard method of extracting and analyzing the sequence of RR intervals recommended in Ref. [3]. The method allows one to pass from the study of a continuous ECG signal to the study of a discrete sequence of RR intervals, from which information on continuous signals of the autonomic nervous system that modulates the heart rate is extracted. The question of the validity and accuracy of this approach remains open.

In order to prove the validity of using the ACP method for extracting the signal of frequency modulation, we compared it with the standard demodulation method—the heterodyning method, which is mathematically well grounded for narrow-band modulating signals. Heterodyning, also called frequency conversion, is used very widely in radio receivers and communication systems [43], but it is typically not applied to physiological signals. The procedure of this method is shown in Fig. 3.

The signal $h(t)$ can be written as

$$h(t) = \int_{-\infty}^{\infty} \hat{S}(f) e^{i2\pi f t} df, \tag{12}$$

where $\hat{S}(f)$ are complex coefficients of the Fourier transform. As explained before, the power spectrum S_h of the frequency-modulated signal $h(t)$ has a peak at the basic frequency f_h and peaks at the frequencies $f_h \pm n f_m$, Fig. 3. Let us filter the signal $h(t)$ with a high-pass filter with a cutoff frequency $f_1 > f_h$. For an ideal filter, all harmonics with the frequencies $f \leqslant f_1$ have zero power. Then the signal at the filter output can be written as

$$\tilde{h}(t) = \int_{f_1}^{\infty} \hat{S}(f) e^{i2\pi f t} df. \tag{13}$$

Since we know the frequency f_h, we can take the local oscillator generating a harmonic signal

$$g(t) = \cos(2\pi f_h t) = \tfrac{1}{2}(e^{i2\pi f_h t} + e^{-i2\pi f_h t}). \tag{14}$$

Using a signal multiplier, we multiply $\tilde{h}(t)$ and $g(t)$:

$$\tilde{m}(t) = \tilde{h}(t)g(t) = \frac{1}{2}\int_{f_1}^{\infty} \hat{S}(f) e^{i2\pi(f+f_h)t} df$$

$$+ \frac{1}{2}\int_{f_1}^{\infty} \hat{S}(f) e^{i2\pi(f-f_h)t} df. \tag{15}$$

Next, we introduce a new variable r using the change of variables $f = r + f_h$. Then $df/dr = 1$ and $df = dr$, and Eq. (15) can be rewritten as follows:

$$\tilde{m}(t) = \frac{1}{2}\int_{f_1-f_h}^{\infty} \hat{S}(r+f_h) e^{i2\pi(r+2f_h)t} dr$$

$$+ \frac{1}{2}\int_{f_1-f_h}^{\infty} \hat{S}(r+f_h) e^{i2\pi r t} dr. \tag{16}$$

The power spectrum of the signal $\tilde{m}(t)$ has peaks at the frequencies $2 f_h + n f_m$ and $n f_m$, Fig. 3. We filter the signal $\tilde{m}(t)$ with a low-pass filter with a cutoff frequency $f_2 < f_h$. At
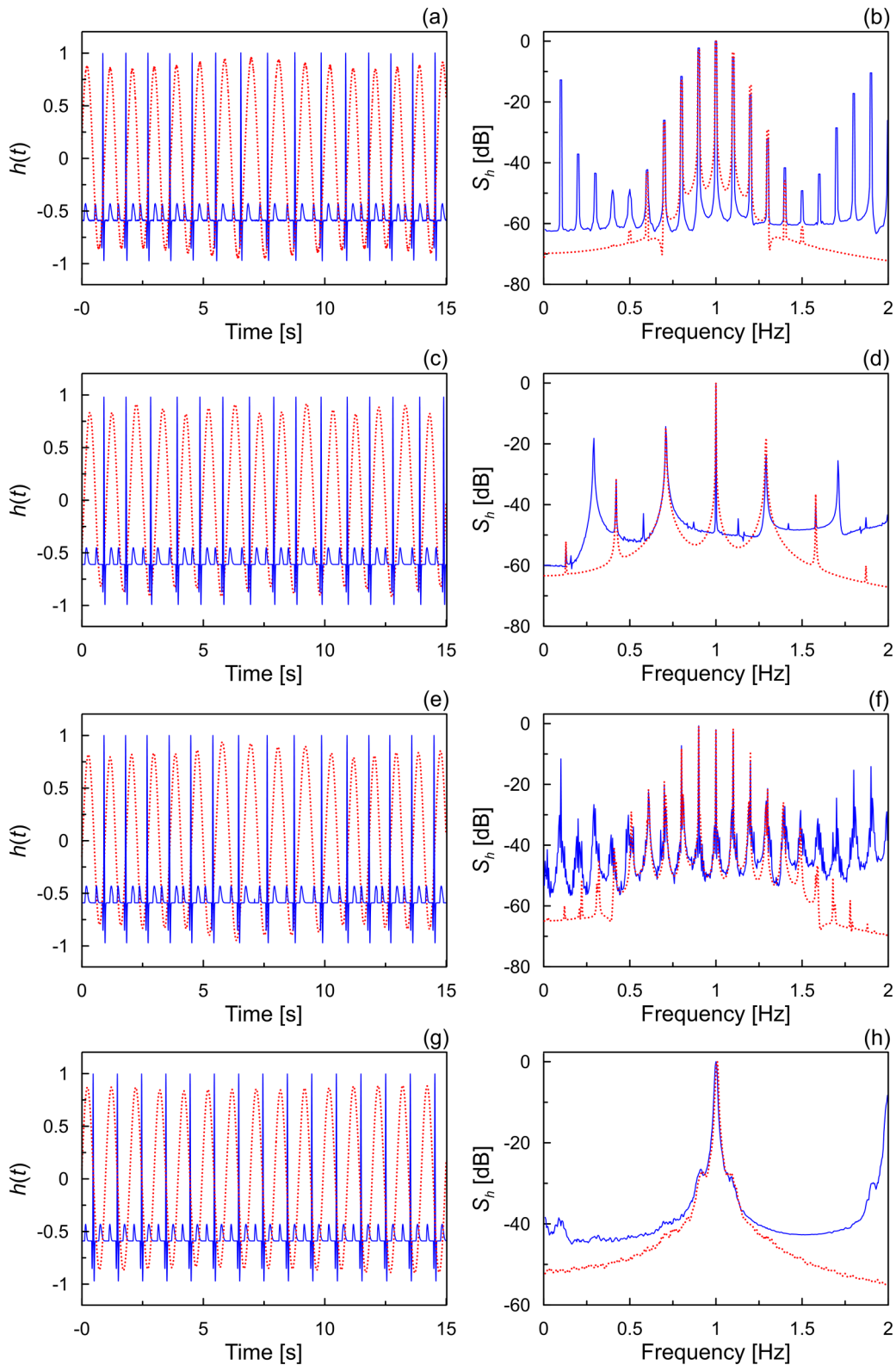
FIG. 2. Time series (left column) and power spectra (right column) of the signals $h(t)$ of the Van der Pol oscillator (6) (dotted red line) and the model of ECG signal (7) (blue line). (a), (b) The case of harmonic modulating signal with $f_m = 0.1$ Hz; (c), (d) the case of harmonic modulating signal with $f_m = 0.29$ Hz; (e), (f) the case of two-frequency modulating signal with $f_{m1} = 0.1$ Hz and $f_{m2} = 0.29$ Hz; (g), (h) the case of broadband modulating signal.
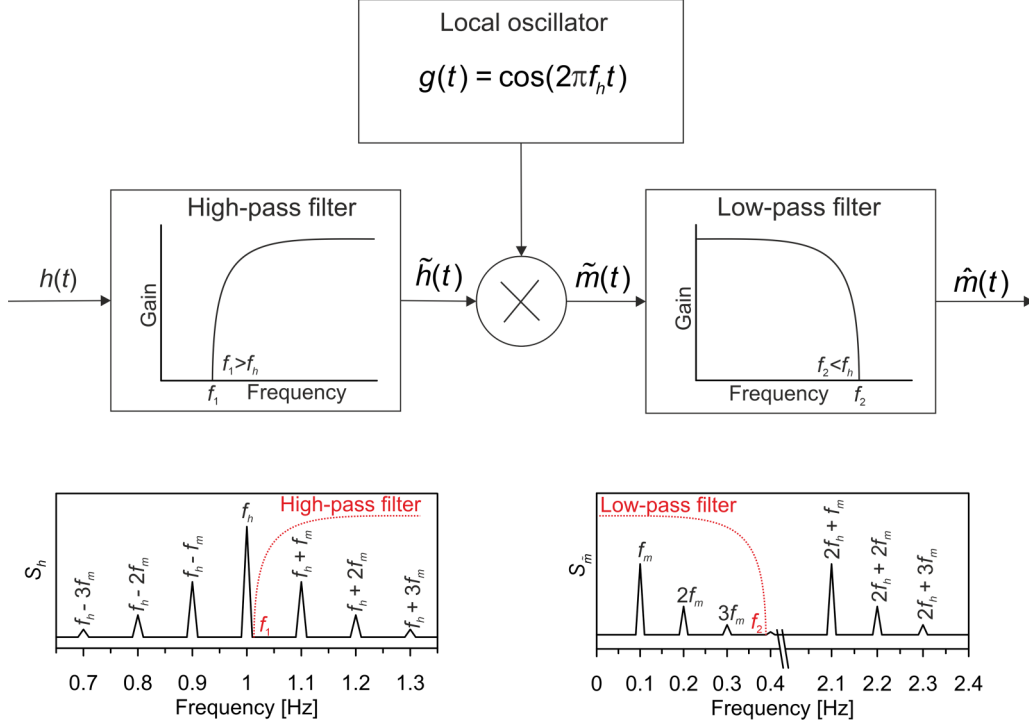
FIG. 3. Scheme of extracting the signal of frequency modulation using the heterodyning technique. $h(t)$ is a frequency-modulated signal, S_h is the power spectrum of $h(t)$, $\tilde{h}(t)$ is the filtered signal $h(t)$, $g(t)$ is a local oscillator signal, $\otimes$ is a signal multiplier, $\tilde{m}(t) = \tilde{h}(t)g(t)$, $S_{\tilde{m}}$ is the power spectrum of $\tilde{m}(t)$, and $\hat{m}(t)$ is the filtered signal $\tilde{m}(t)$.

the output of the filter, we get the signal

$$\hat{m}(t) = \frac{1}{2} \int_{f_1-f_h}^{f_2} \hat{S}(r + f_h)e^{i2\pi(r+2f_h)t}dr$$
$$+ \frac{1}{2} \int_{f_1-f_h}^{f_2} \hat{S}(r + f_h)e^{i2\pi rt}dr. \tag{17}$$

Since $f_2 < f_h$ (see Fig. 3), the first term of Eq. (17) is always zero due to filtering. Then Eq. (17) can be written as

$$\hat{m}(t) = \frac{1}{2} \int_{f_1-f_h}^{f_2} \hat{S}(r + f_h)e^{i2\pi rt}dr. \tag{18}$$

Thus, heterodyning allows one to shift one frequency range into another, a new frequency range, and can be used for demodulation [43]. In the simplest case, if $r = f_m$, then $f = f_h + f_m$, and as a result of heterodyning, we obtain a difference frequency $(f - f_h) = f_m$, which is the frequency of modulation.

To study the quality of extraction of the modulating signal $m(t)$ from the frequency-modulated signal $h(t)$ using the methods of ACP and heterodyning, we carried out a frequency response analysis. To calculate the amplitude response (AR) and phase response (PR) of the studied systems, we varied the frequency of the harmonic modulating signal (3) with a step of 0.01 Hz and, at each step, found the amplitude ratio and phase difference of the signals $\hat{m}(t)$ and $m(t)$, respectively. The AR and PR curves plotted for both studied oscillators for both cases of extracting the signal $\hat{m}(t)$ using ACP method or heterodyning technique are shown in Sec. IV.

IV. RESULTS

We compare the time series and power spectra of modulating signals $m(t)$ with the time series and power spectra of signals $\hat{m}(t)$ extracted from the frequency-modulated signals $h(t)$ of the Van der Pol oscillator (6) and the model of ECG signal (7) using the methods of ACP and heterodyning. The obtained results are presented below for the three different types of modulating signals $m(t)$.

Figure 4 illustrates the case of harmonic signal $m(t)$, which is described by Eq. (3) and has the frequency $f_m = 0.1$ Hz. Figure 4(a) shows the time series of the signals $\hat{m}(t)$ extracted from the signal $h(t)$ of the Van der Pol oscillator using either the ACP method or the heterodyning technique. The signals $\hat{m}(t)$ are close to periodic. Their period coincides with the period of the signal $m(t)$, but the amplitude is slightly less than that of $m(t)$. In the power spectra of the signals $\hat{m}(t)$, the main peak is observed at $f = f_m = 0.1$ Hz, Fig. 4(b). In addition to the main peak, the spectra of $\hat{m}(t)$ have peaks at higher harmonics, which appear due to the nonlinearity of the oscillator. Qualitatively similar results are obtained for the model of ECG signal, Figs. 4(c) and 4(d).

The case of the harmonic modulating signal $m(t)$ with the frequency $f_m = 0.29$ Hz is presented in Fig. 5. The signals $\hat{m}(t)$ in Figs. 5(a) and 5(c) differ more from the signal $m(t)$ than at $f_m = 0.1$ Hz [see Figs. 4(a) and 4(c)]. The period of the signals $\hat{m}(t)$ is the same as the period of $m(t)$, but the amplitude is noticeably smaller. The main peak in the power spectra of $\hat{m}(t)$ is observed at $f = f_m = 0.29$ Hz, Figs. 5(b) and 5(d). In addition to the main peak, the spectra of $\hat{m}(t)$ have a subharmonic peak. Thus, in the case of harmonic modulation
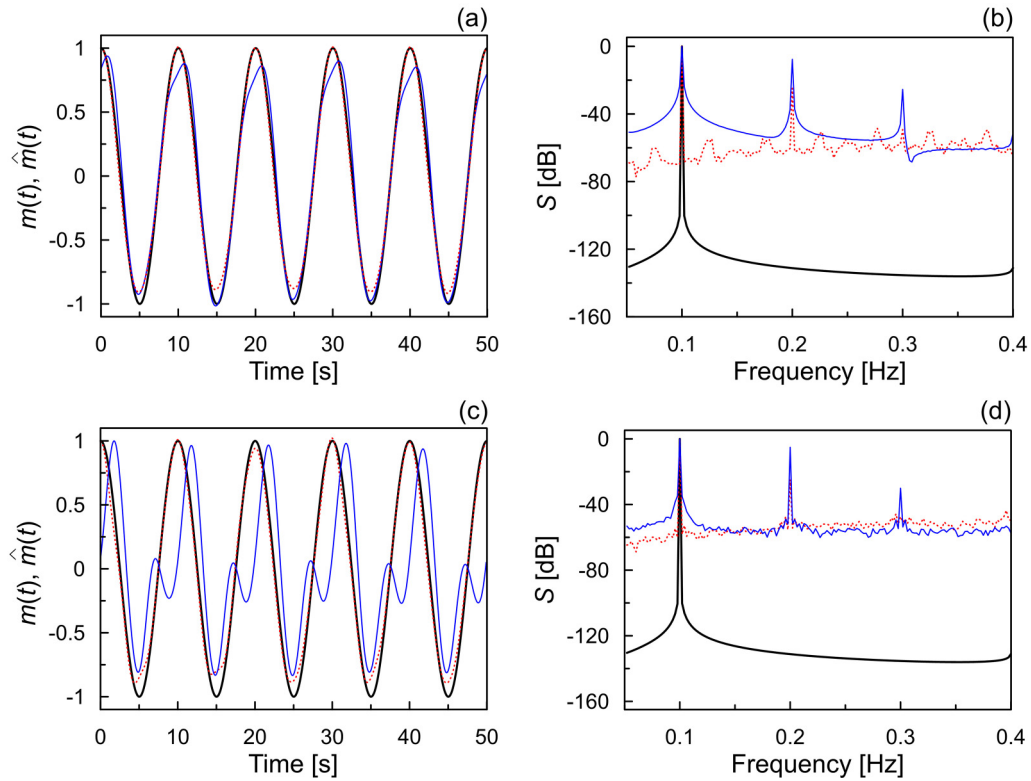
FIG. 4. Time series (left column) and power spectra (right column) of the harmonic modulating signal $m(t)$ with the frequency $f_m = 0.1$ Hz (bold black line), the signal $\hat{m}(t)$ extracted using the ACP approach (dotted red line), and the signal $\hat{m}(t)$ extracted using the heterodyning technique (thin blue line). (a), (b) The signals $\hat{m}(t)$ are extracted from the signal $h(t)$ of the Van der Pol oscillator. (c), (d) The signals $\hat{m}(t)$ are extracted from the signal $h(t)$ of the model of ECG signal.

of the oscillator frequency, it is possible to extract the modulating signal from the observed frequency-modulated signal with good accuracy. With simple model examples of harmonic modulation of the oscillator frequency, the ACP method has shown results that are similar to those of the mathematically well grounded heterodyning method, Figs. 4 and 5, which indicate that the ACP method is an effective method of demodulation.

Figure 6 shows the results of extraction of the signals $\hat{m}(t)$ for the case of two-frequency modulating signal $m(t)$ described by Eq. (10) with $A_1 = 1$, $f_{m1} = 0.1$ Hz, $A_2 = 0.16$, and $f_{m2} = 0.29$ Hz. The time series of the signals $\hat{m}(t)$ extracted by both methods differ from the time series of $m(t)$, Figs. 6(a) and 6(c). However, the power spectra of the signals $\hat{m}(t)$ show peaks at the frequencies of 0.1 and 0.29 Hz, which coincide with the frequencies of the signal $m(t)$, Figs. 6(b) and 6(d). In the spectra of the signals $\hat{m}(t)$, there are also peaks at higher harmonics and at combination frequencies.

Figure 7 illustrates the case of a broadband modulating signal $m(t)$, the time series of which is nonperiodic. The time series of $m(t)$ and $\hat{m}(t)$ are not similar to each other, Figs. 7(a) and 7(c). Nevertheless, the ACP method allows us to obtain the signal $\hat{m}(t)$, whose power spectrum is similar to that of the modulating signal $m(t)$, Figs. 7(b) and 7(d). The spectra are particularly similar in the LF range, while in the HF range, the power of the signal $\hat{m}(t)$ is slightly underestimated. Note that the heterodyning technique did not allow us to obtain the signal $\hat{m}(t)$, the spectrum of which is similar to the spectrum of the signal $m(t)$.

It follows from our results that time series of the modulating signal can be reconstructed quite accurately from the frequency-modulated signal $h(t)$ only if the modulating signal $m(t)$ is harmonic. However, spectral properties of the signal $m(t)$ can be evaluated from the signal $h(t)$ even in the case of complex modulating signals. In the case of two-frequency modulation, the ACP method provides a better assessment of the signal $m(t)$ spectrum than the heterodyning technique. In the case of broadband modulation, the heterodyning technique was not suitable for assessing the spectrum of the modulating signal $m(t)$, since this method is intended for narrow-band modulating signals.

In the case of broadband frequency modulation of the signal $h(t)$, the multiplication of signals in Eq. (15) and subsequent filtering lead to the absence of pronounced peaks in the power spectrum of the signal $\hat{m}(t)$ extracted using the heterodyning technique, Figs. 7(b) and 7(d). In contrast to the heterodyning method, which works with continuous signals, the ACP method extracts a discrete sequence of oscillation period values from the frequency-modulated signal $h(t)$. A subsequent interpolation of this sequence and bandpass filtering of the obtained signal allows one to assess the spectral properties of even a broadband modulating signal. Thus, for the ACP method, the broadband frequency modulation is less critical than for the heterodyning technique.

As noted above, the signals of the autonomic nervous system that regulate the heart rate are broadband. Based on our numerical model studies, it can be concluded that the LF and HF components of HRV, which are typically obtained from
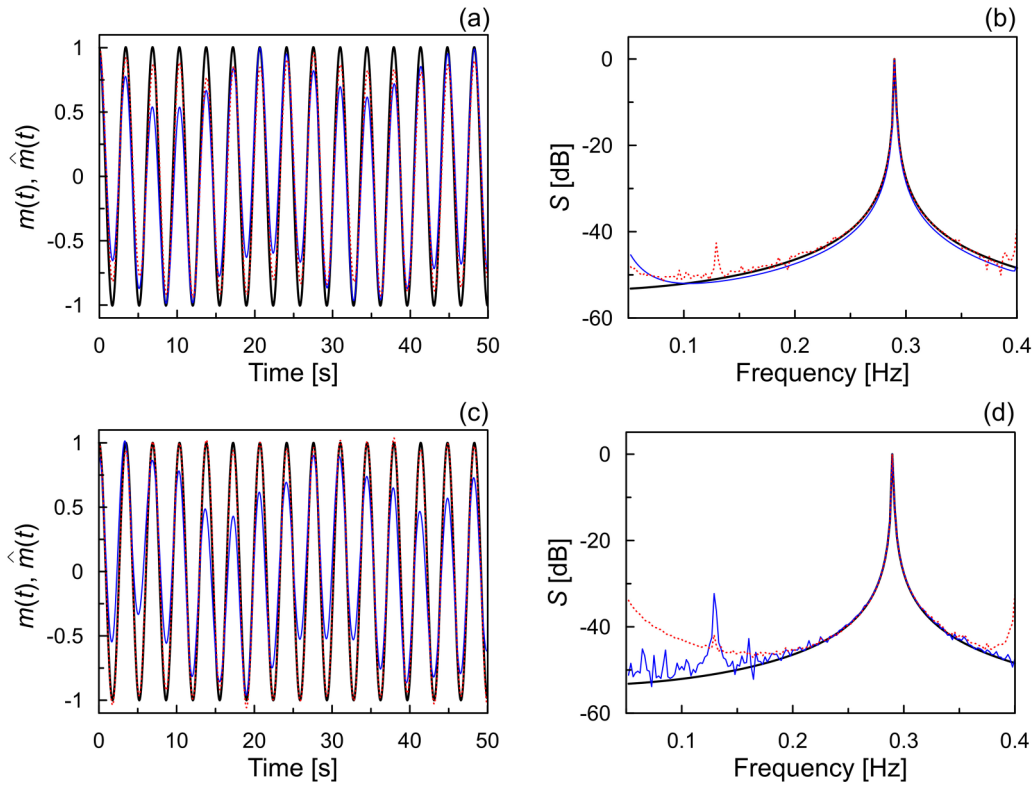
FIG. 5. Time series (left column) and power spectra (right column) of the harmonic modulating signal $m(t)$ with the frequency $f_m = 0.29$ Hz (bold black line), the signal $\hat{m}(t)$ extracted using the ACP approach (dotted red line), and the signal $\hat{m}(t)$ extracted using the heterodyning technique (thin blue line). (a), (b) The signals $\hat{m}(t)$ are extracted from the signal $h(t)$ of the Van der Pol oscillator. (c), (d) The signals $\hat{m}(t)$ are extracted from the signal $h(t)$ of the model of ECG signal.

ECG using the analysis of RR intervals (i.e., by the ACP method), can differ strongly from the signals of frequency modulation of the heart rate in shape, but have close similarity with them in the frequency domain. The characteristics of RR intervals in the time domain are widely used in medicine and have proven diagnostic value. The results of our study indicate only that the time series of LF and HF oscillations in HRV, in the general case, significantly differ from the time series of modulating signals reflecting the activity of the autonomic nervous system.

Figure 8 shows the amplitude response (AR) curves and phase response (PR) curves for both studied oscillators, which were plotted using the ACP and heterodyning methods for the extraction of harmonic modulating signal. For the Van der Pol oscillator and the model of ECG signal, we obtained qualitatively similar AR and PR curves using the ACP method for extracting the signal $\hat{m}(t)$, Figs. 8(a) and 8(c). In both plots, the AR curves monotonically decrease with increasing frequency. Such AR is typical for a low-pass low-order filter. The PR curves are linear in both plots, Figs. 8(a) and 8(c). According to these results, the ACP method allows one to more accurately extract the LF modulating signals than the HF modulating signals. This is in good agreement with Figs. 4(a), 4(c), 5(a), and 5(c). Figures 8(b) and 8(d) show the AR and PR curves for the case of the signal $m(t)$ extraction using the heterodyning technique. These curves indicate that the heterodyning technique significantly distorts the signal $\hat{m}(t)$ in comparison with $m(t)$, especially at higher frequencies. Compared to the ACP method, the heterodyning technique

turns out to be less accurate in extracting the signal of frequency modulation in the considered examples. Note that, by construction, the frequency response curves in Fig. 8 allow us to analyze only the case of harmonic modulation.

As seen from Fig. 8, when extracting the modulating signal from the frequency-modulated signal using the ACP and heterodyning methods, both the amplitude and the phase of the signal are distorted. As a result, the amplitude and phase of the extracted signal $\hat{m}(t)$ differ from the amplitude and phase of the modulating signal $m(t)$. Therefore, in Figs. 7(a) and 7(c), the time series differ from each other. However, the power spectra of the signal $m(t)$ and the signal $\hat{m}(t)$ extracted using the ACP approach are similar in Figs. 7(b) and 7(d). In Ref. [45] it was shown that signals can have the same power spectra, despite the difference in their time series.

The considered frequency-modulated Van der Pol oscillator (6) certainly does not pretend to describe the electrical activity of the human heart. Even the dynamical model of ECG signal (7), which is capable of replicating many of the important features of the human ECG, is still only an approximation of real ECG signals. Real signals that modulate the heart rate are also more complex in shape than the model signals $m(t)$ that we have considered. For these reasons, the signals $\hat{m}(t)$ extracted from the experimental ECG and representing the sequence of RR intervals differ from the signals $\hat{m}(t)$ plotted in Figs. 4–7 using the model data. The power spectra of signals $\hat{m}(t)$ extracted from experimental and model frequency-modulated signals also differ.
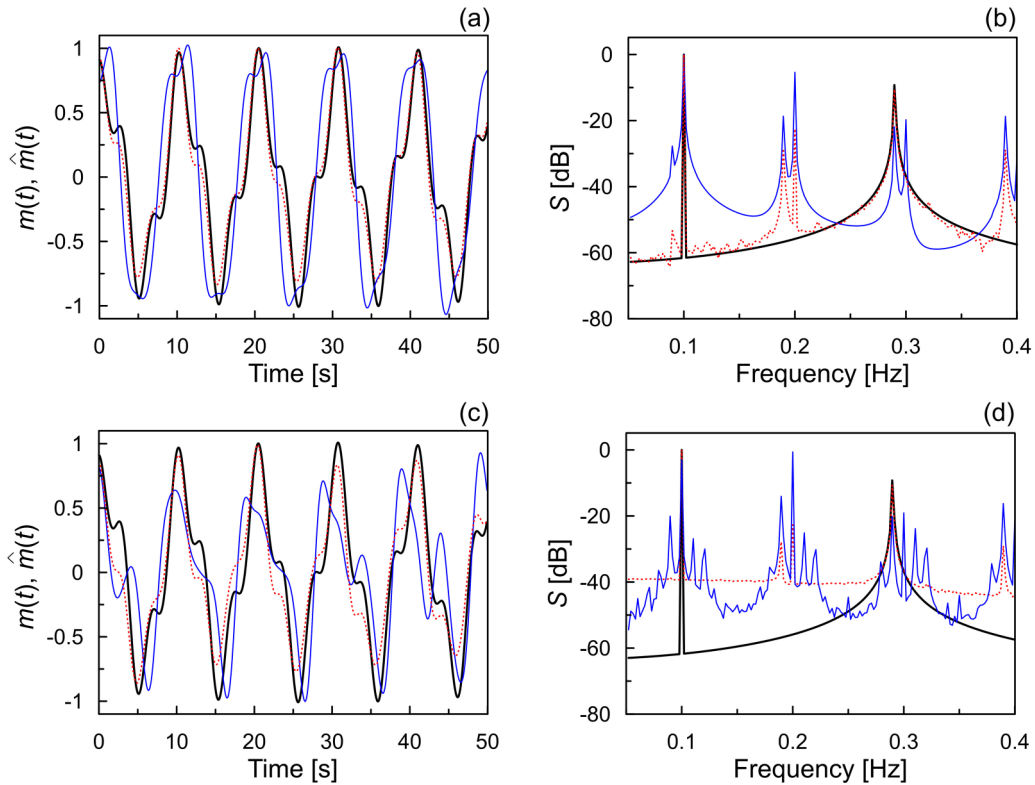
FIG. 6. Time series (left column) and power spectra (right column) of the two-frequency modulating signal $m(t)$ with the frequencies $f_{m1} = 0.1$ Hz and $f_{m2} = 0.29$ Hz, and the amplitudes $A_1 = 1$ and $A_2 = 0.16$ (bold black line), the signal $\hat{m}(t)$ extracted using the ACP approach (dotted red line), and the signal $\hat{m}(t)$ extracted using the heterodyning technique (thin blue line). (a), (b) The signals $\hat{m}(t)$ are extracted from the signal $h(t)$ of the Van der Pol oscillator. (c), (d) The signals $\hat{m}(t)$ are extracted from the signal $h(t)$ of the model of ECG signal.

We studied ten healthy subjects (five males and five females) aged 20–25 years. All subjects gave written consent to participate in the study. ECG signals were recorded in a supine resting condition under spontaneous breathing. The duration of each record was 2 h. The signals were recorded with a 14-bit resolution and sampling frequency of 250 Hz, which corresponds to a sampling time of 0.004 s equal to the integration step Δt used in the numerical study of oscillators (6) and (7). Figure 9(a) shows typical time series of the signals $\hat{m}(t)$ extracted from the experimental ECG of a healthy subject using either the ACP method or the heterodyning technique. Figure 9(b) shows the power spectra of these signals. In fact, the dotted red line in Fig. 9(b) depicts the power spectrum of a real sequence of RR intervals obtained in a standard way [3] from the experimental ECG signal. Figure 9(c) shows the power spectra of the signals $\hat{m}(t)$ averaged over the entire group of ten subjects.

Figure 9 is most similar to Fig. 7, plotted for the case of broadband modulation of model oscillators. When analyzing real ECG signals, the heterodyning method turned out to be ineffective. However, it can be expected to be effective when ECG signals have narrower and higher peaks in the LF and HF ranges. In contrast to the heterodyning technique, the ACP method allowed us to obtain characteristic peaks in the HRV power spectrum in Fig. 9(b) associated with sympathetic and parasympathetic modulation of the heart rate. Unfortunately, we cannot compare the time series and their spectra presented in Fig. 9 with the time series and spectra of real

signals from the autonomic nervous system modulating the heart rate, since invasive methods are required to obtain these signals.

Nevertheless, without invasive measurements, it can be shown that the powers of the LF and HF components of HRV are associated with the activity of the autonomic nervous system. For this, different approaches are used, for example, a tilt table test, otherwise known as a "passive stand," [46]. In the tilt table test, the patient first lies strapped to a tilt table for about 20 min, and then the table is tilted from a horizontal position to an upright position, which is maintained for about 10 min. Normally, upon tilt up there is an increase in the sympathetic activity and a decrease in the parasympathetic activity of the autonomic nervous system [46,47], which is manifested in a change of the power spectrum of RR intervals.

We carried out a tilt table test with two young healthy subjects. Figure 10 shows the power spectra of sequences of RR intervals for both subjects who first lay flat on a table and then tilted upright. According to the terminology we have introduced, these are the power spectra of the signals $\hat{m}(t)$ extracted from the ECG signals using the ACP approach. It can be seen in Fig. 10 that in the upright position, the power of the LF component of HRV associated with sympathetic modulation of the heart rate increased, while the power of the HF component of HRV associated with parasympathetic modulation decreased. This result is in good agreement with the known results [46,47].
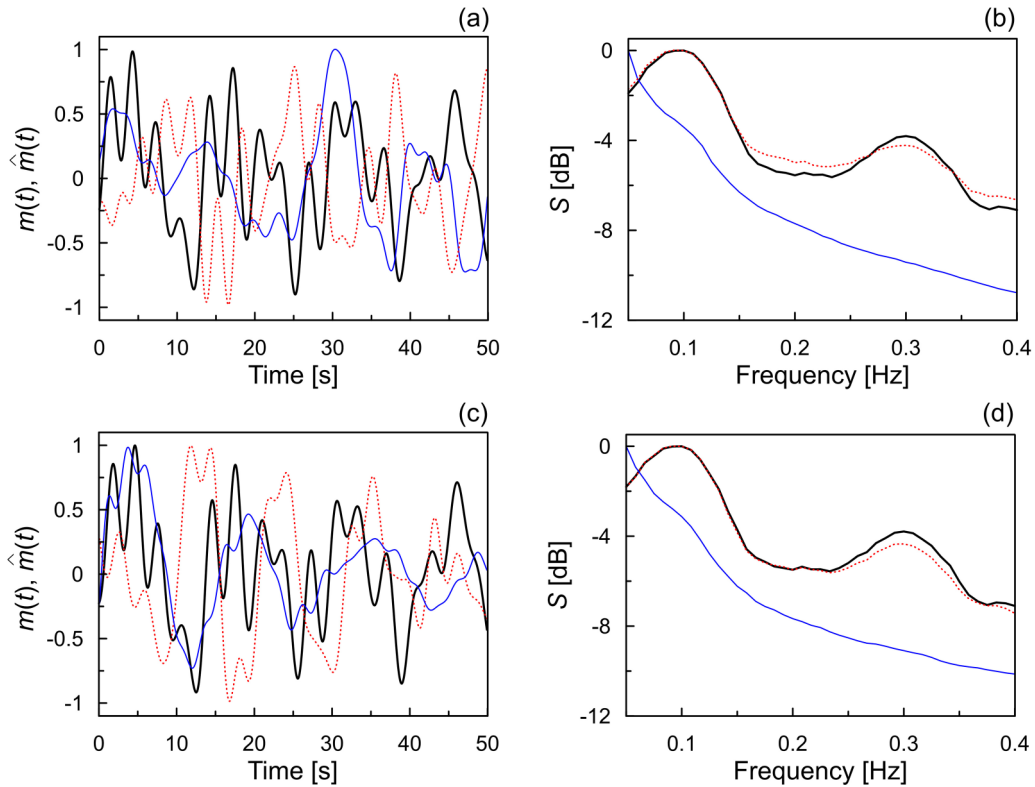
FIG. 7. Time series (left column) and power spectra (right column) of the broadband modulating signal $m(t)$ (bold black line), the signal $\hat{m}(t)$ extracted using the ACP approach (dotted red line), and the signal $\hat{m}(t)$ extracted using the heterodyning technique (thin blue line). (a), (b) The signals $\hat{m}(t)$ are extracted from the signal $h(t)$ of the Van der Pol oscillator. (c), (d) The signals $\hat{m}(t)$ are extracted from the signal $h(t)$ of the model of ECG signal.

Limitations. The study of the possibility of extracting the signal of frequency modulation from a frequency-modulated signal was carried out in our paper using only two mathematical models. One of them is the frequency-modulated Van der Pol oscillator, which does not pretend to describe the electrical activity of the human heart. The second model is the dynamical model of ECG signal, which is only an approximation of real ECG signals. We did not consider the cases of various ECG wave forms associated with the individual characteristics of patients and pathologies of the cardiovascular system. In particular, the presence of cardiac arrhythmias can affect the results of the study. Moreover, real signals that modulate the heart rate are more complex in shape than the model signals $m(t)$ that we have considered. The heterodyning technique is intended for narrow-band modulating signals, so it turned out to be ineffective in the case of broadband frequency modulation. Finally, we did not have invasive signals that directly characterize the activity of the autonomic nervous system. This did not allow us to compare the time series and their spectra presented in Fig. 9 with the time series and spectra of real signals modulating the heart rate.

V. CONCLUSION

Using two model oscillators with frequency modulation, we have investigated the possibility of extracting the signal of frequency modulation under the assumption that only the oscillator signal is available for analysis. We have shown

that, using the ACP and heterodyning methods, it is possible to quite accurately extract the modulating signal only in the case of harmonic modulation of the oscillator frequency, but the accuracy of both methods decreases with an increasing frequency of modulation. With more complex modulating signals, the quality of reconstruction of their time series is significantly reduced, what can be explained by the nonlinearity of the oscillator. However, the main frequency components of the modulating signal can be reconstructed even in the case of broadband modulation of the oscillator frequency.

For real human ECG signals, whose frequency is modulated by the autonomic nervous system, the obtained results can be interpreted as follows. The time series of LF and HF oscillations in HRV that are extracted from ECG using the analysis of RR intervals, in the general case, significantly differ from the time series of the signals of frequency modulation of the heart rate. However, the power spectrum of RR intervals in the LF and HF bands has peaks at the same frequencies as the signals of frequency modulation. The quality of extracting the LF component of HRV associated with sympathetic modulation of the heart rate by the autonomic nervous system is higher than the quality of extracting the HF component of HRV associated with parasympathetic modulation.

The nonlinearity inherent in both the heart and the autonomic nervous system, the complex interaction between these systems, and the influences of noise lead to a more complicated response of the heart to the activity of the autonomic nervous system than a simple frequency
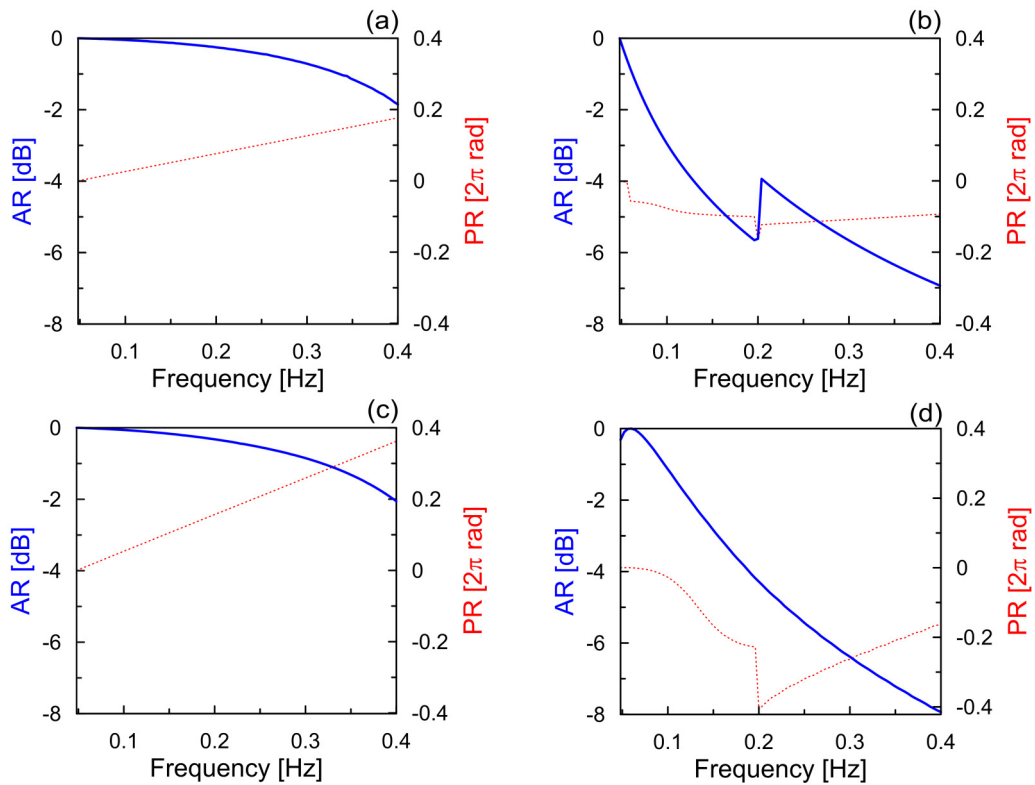
FIG. 8. Amplitude response curves (blue line) and phase response curves (dotted red line) of the Van der Pol oscillator (a), (b) and the model of ECG signal (c), (d) plotted using the ACP approach (a), (c) and heterodyning technique (b), (d) for the extraction of harmonic modulating signal.
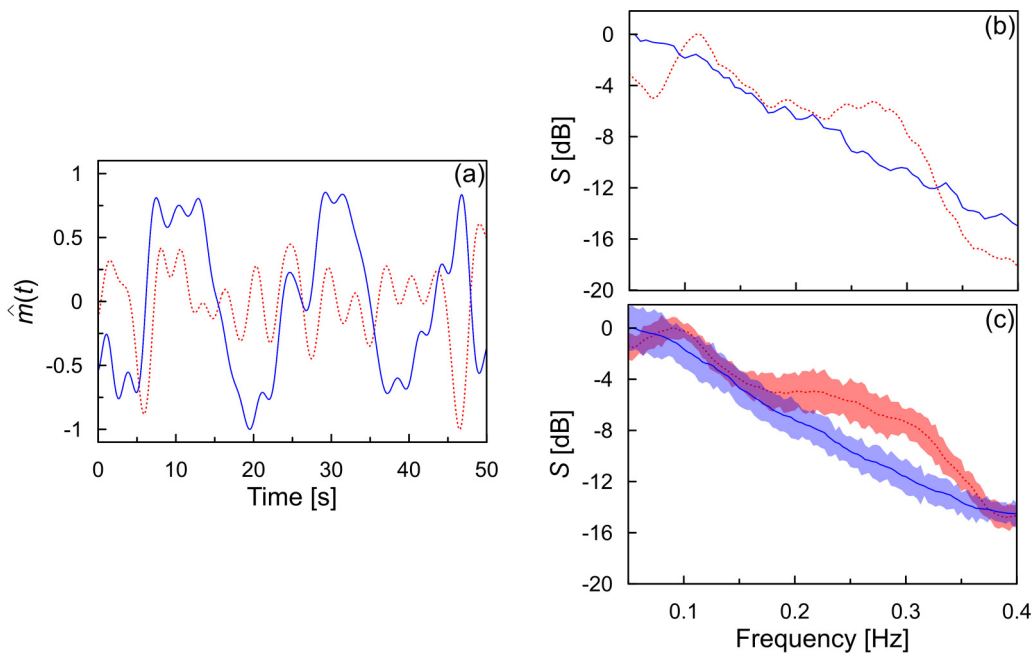

FIG. 9. Time series (a) and power spectra (b) of the signals $\hat{m}(t)$ extracted from the experimental ECG using the ACP approach (dotted red line) and the heterodyning technique (blue line). (c) Power spectra of the signals $\hat{m}(t)$ averaged over the entire group of 10 subjects. For the ACP method, the mean S values and their standard errors are shown by the dotted red line and pink, respectively, and for the heterodyning method, by the blue line and light blue, respectively.
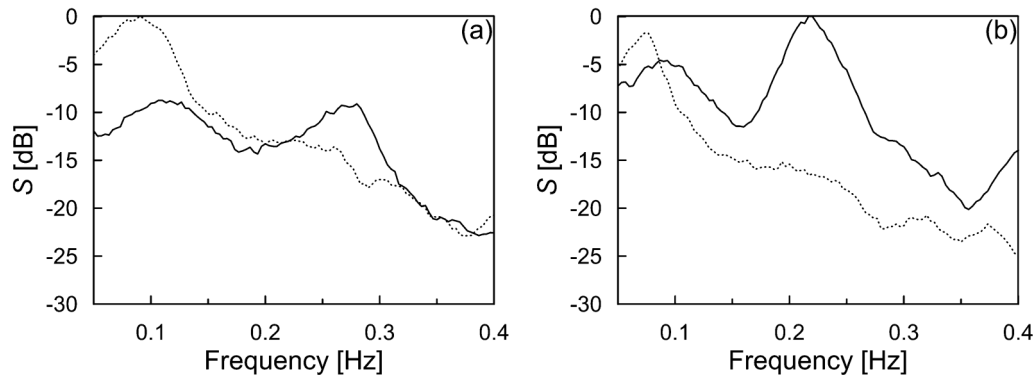
FIG. 10. Power spectra of the signals $\hat{m}(t)$ extracted from the experimental ECG signals using the ACP approach for a subject lying flat (solid line) and then tilted upright (dotted line). (a) Subject A; (b) subject B.

modulation of the heart rate. Thus, the LF and HF components of HRV should be used with caution as estimates of the sympathetic and parasympathetic activity modulating the heart rate.

Since the activity of the autonomic nervous system contains important information for medical diagnostics, its adequate assessment using easily available ECG signals is of great interest. However, for a more accurate answer to the question of how well the interbeat interval variability reflects the frequency modulation of the heart rate, the next step is to move from analyzing model data to analyzing real data. This will require recording not only ECG signals, but also invasive measurement of signals characterizing the activity of the autonomic nervous system.

[1] O. Monfredi, H. Dobrzynski, T. Mondal, M. R. Boyett, and G. M. Morris, The anatomy and physiology of the sinoatrial node—A contemporary review, Pacing Clin. Electrophysiol. **33**, 1392 (2010).

[2] J. Jalife and D. C. Michaels, Neural control of sinoatrial pacemaker activity, in *Vagal Control of the Heart: Experimental Basis and Clinical Implications*, edited by M. N. Levy, and P. J. Schwartz (Futura, Armonk, NY, 1994), p. 173.

[3] A. J. Camm, M. Malik, J. T. Bigger, G. Breithardt, S. Cerutti, R. J. Cohen, P. Coumel, E. L. Fallen, H. L. Kennedy, R. E. Kleiger, F. Lombardi, A. Malliani, A. J. Moss, J. N. Rottman, G. Schmidt, P. J. Schwartz, and D. H. Singer, Task Force of the European Society of Cardiology and the North American Society of Pacing and Electrophysiology, Heart rate variability: Standards of measurement, physiological interpretation, and clinical use, Circulation **93**, 1043 (1996).

[4] A. Malliani, M. Pagani, F. Lombardi, and S. Cerutti, Cardiovascular neural regulation explored in the frequency domain, Circulation **84**, 482 (1991).

[5] J. A. Hirsch and B. Bishop, Respiratory sinus arrhythmia in humans: How breathing pattern modulates heart rate, Am. J. Physiol. Heart Circ. Physiol. **241**, H620 (1981).

[6] M. Moser, M. Lehofer, A. Sedminek, M. Lux, H. G. Zapotoczky, T. Kenner, and A. Noordergraaf, Heart rate variability as a prognostic tool in cardiology. A contribution to the problem from a theoretical point of view, Circulation **90**, 1078 (1994).

[7] P. Grossman and E. W. Taylor, Toward understanding respiratory sinus arrhythmia: Relations to cardiac vagal tone,

evolution and biobehavioral functions, Biol. Psychol. **74**, 263 (2007).

[8] T. Ritz, M. Bosquet Enlow, S. M. Schulz, R. Kitts, J. Staudenmayer, and R. J. Wright, Respiratory sinus arrhythmia as an index of vagal activity during stress in infants: Respiratory influences and their control, PLoS One **7**, e52729 (2012).

[9] P. Graziano and K. Derefinko, Cardiac vagal control and children's adaptive functioning: A meta-analysis, Biol. Psychol. **94**, 22 (2013).

[10] G. F. Lewis, S. A. Furman, M. F. McCool, and S. W. Porges, Statistical strategies to quantify respiratory sinus arrhythmia: Are commonly used metrics equivalent? Biol. Psychol. **89**, 349 (2012).

[11] P. H. Charlton, D. A. Birrenkott, T. Bonnici, M. A. F. Pimentel, A. E. W. Johnson, J. Alastruey, L. Tarassenko, P. J. Watkinson, R. Beale, and D. A. Clifton, Breathing rate estimation from the electrocardiogram and photoplethysmogram: A review, IEEE Rev. Biomed. Eng. **11**, 2 (2018).

[12] J. Kuo and Ch.-D. Kuo, Decomposition of heart rate variability spectrum into a power-law function and a residual spectrum, Front. Cardiovasc. Med. **3**, 16 (2016).

[13] M. D. Prokhorov, V. I. Ponomarenko, V. I. Gridnev, M. B. Bodrov, and A. B. Bespyatov, Synchronization between main rhythmic processes in the human cardiovascular system, Phys. Rev. E **68**, 041913 (2003).

[14] V. I. Ponomarenko, M. D. Prokhorov, A. B. Bespyatov, M. B. Bodrov, and V. I. Gridnev, Deriving main rhythms of the human cardiovascular system from the heartbeat time series

and detecting their synchronization, Chaos Solitons Fractals **23**, 1429 (2005).

[15] R. B. Pachoria, P. Avinash, K. Shashank, R. Sharma, and U. R. Acharya, Application of empirical mode decomposition for analysis of normal and diabetic RR-interval signals, Expert Syst. Appl. **42**, 4567 (2015).

[16] M. Bracic Lotric, A. Stefanovska, D. Stajer, and V. Urbancic-Rovan, Spectral components of heart rate variability determined by wavelet analysis, Physiol. Meas. **21**, 441 (2000).

[17] B. Kralemann, M. Frühwirth, A. Pikovsky, M. Rosenblum, T. Kenner, J. Schaefer, and M. Moser, In vivo cardiac phase response curve elucidates human respiratory heart rate variability, Nat. Commun. **4**, 2418 (2013).

[18] Ç. Topçu, M. Frühwirth, M. Moser, M. Rosenblum, and A. Pikovsky, Disentangling respiratory sinus arrhythmia in heart rate variability records, Physiol. Meas. **39**, 054002 (2018).

[19] G. Parati, G. Mancia, M. D. Rienzo, P. Castiglioni, J. A. Taylor, and P. Studinger, Point:Counterpoint: Cardiovascular variability is/is not an index of autonomic control of circulation, J. Appl. Physiol. **101**, 676 (2006).

[20] A. Malliani, C. Julien, G. E. Billman, S. Cerutti, M. F. Piepoli, L. Bernardi, P. Sleight, M. A. Cohen, C. O. Tan, D. Laude, M. Elstad, K. Toska, J. M. Evans, and D. L. Eckberg, Point:Counterpoint Comments, J. Appl. Physiol. **101**, 684 (2006).

[21] M. Pagani, N. Montano, A. Porta, A. Malliani, F. M. Abboud, C. Birkett, and V. K. Somers, Relationship between spectral components of cardiovascular variabilities and direct measures of muscle sympathetic nerve activity in humans, Circulation **95**, 1441 (1997).

[22] N. Montano, T. Gnecchi-Ruscone, A. Porta, F. Lombardi, A. Malliani, and S. M. Barman, Presence of vasomotor and respiratory rhythms in the discharge of single medullary neurons involved in the regulation of cardiovascular system, J. Auton. Nerv. Syst. **57**, 116 (1996).

[23] R. L. Cooley, N. Montano, C. Cogliati, P. van de Borne, W. Richenbacher, R. Oren, and V. K. Somers, Evidence for a central origin of the low-frequency oscillation in RR-interval variability, Circulation **98**, 556 (1998).

[24] R. W. DeBoer, J. W. Karemaker, and J. Stracke, Hemodynamic fluctuations and baroreflex sensitivity in humans: A beat-to-beat model, Am. J. Physiol. Heart Circ. Physiol. **253**, H680 (1987).

[25] L. Bernardi, S. Leuzzi, A. Radaelli, C. Passino, J. A. Johnston, and P. Sleight, Low-frequency spontaneous fluctuations of R-R interval and blood pressure in conscious humans: A baroreceptor or central phenomenon? Clin. Sci. **87**, 649 (1994).

[26] S. Malpas, Neural influences on cardiovascular variability: Possibilities and pitfalls, Am. J. Physiol. Heart Circ. Physiol. **282**, H6 (2002).

[27] G. Eisenhofer, P. Friberg, B. Rundqvist, A. A. Quyyumi, G. Lambert, D. M. Kaye, I. J. Kopin, D. S. Goldstein, and M. D. Esler, Cardiac sympathetic nerve function in congestive heart failure, Circulation **93**, 1667 (1996).

[28] A. J. McCance, P. A. Thompson, and J. C. Forfar, Increased cardiac sympathetic nervous activity in patients with unstable coronary heart disease, Eur. Heart. J. **14**, 751 (1993).

[29] S. Julius and S. Nesbitt, Sympathetic overactivity in hypertension. A moving target, Am. J. Hypertens. **9**, 113S (1996).

[30] D. Lucini, Impairment in cardiac autonomic regulation preceding arterial hypertension in humans: Insights from spectral analysis of beat-by-beat cardiovascular variability, Circulation **106**, 2673 (2002).

[31] B. W. Hyndman, R. I. Kitney, and B. M. Sayers, Spontaneous rhythms in physiological control systems, Nature (London) **233**, 339 (1971).

[32] S. D. Akselrod, D. Gordon, J. B. Madwed, N. C. Snidman, D. C. Shannon, and R. J. Cohen, Power spectrum analysis of heart rate fluctuations: A quantitative probe of beat-to-beat cardiovascular control, Science **213**, 220 (1981).

[33] A. S. Karavaev, M. D. Prokhorov, V. I. Ponomarenko, A. R. Kiselev, V. I. Gridnev, E. I. Ruban, and B. P. Bezruchko, Synchronization of low-frequency oscillations in the human cardiovascular system, Chaos **19**, 033112 (2009).

[34] A. R. Kiselev, V. I. Gridnev, M. D. Prokhorov, A. S. Karavaev, O. M. Posnenkova, V. I. Ponomarenko, B. P. Bezruchko, and V. A. Shvartz, Evaluation of 5-year risk of cardiovascular events in patients after acute myocardial infarction using synchronization of 0.1-Hz rhythms in cardiovascular system, Ann. Noninvasive. Electrocardiol. **17**, 204 (2012).

[35] V. I. Ponomarenko, M. D. Prokhorov, A. S. Karavaev, A. R. Kiselev, V. I. Gridnev, and B. P. Bezruchko, Synchronization of low-frequency oscillations in the cardiovascular system: Application to medical diagnostics and treatment, Eur. Phys. J.: Spec. Top. **222**, 2687 (2013).

[36] A. R. Kiselev, E. I. Borovkova, V. A. Shvartz, V. V. Skazkina, A. S. Karavaev, M. D. Prokhorov, A. Y. Ispiryan, S. A. Mironov, and O. L. Bockeria, Low-frequency variability in photoplethysmographic waveform and heart rate during on-pump cardiac surgery with or without cardioplegia, Sci. Rep. **10**, 2118 (2020).

[37] I. W. Neufeld, A. R. Kiselev, A. S. Karavaev, M. D. Prokhorov, V. I. Gridnev, V. I. Ponomarenko, and B. P. Bezruchko, Autonomic control of cardiovascular system in pre- and post-menopausal women: A cross-sectional study, J. Turk. Ger. Gynecol. Assoc. **16**, 11 (2015).

[38] A. R. Kiselev, V. I. Gridnev, M. D. Prokhorov, A. S. Karavaev, O. M. Posnenkova, V. I. Ponomarenko, and B. P. Bezruchko, Selection of optimal dose of beta-blocker treatment in myocardial infarction patients basing on changes in synchronization between 0.1 Hz oscillations in heart rate and peripheral microcirculation, J. Cardiovasc. Med. **13**, 491 (2012).

[39] D. L. Jardine, H. Ikram, C. M. Frampton, R. Frethey, S. I. Bennett, and I. G. Crozier, Autonomic control of vasovagal syncope, Am. J. Physiol. Heart. Circ. Physiol. **274**, H2110 (1998).

[40] M. Lambertz and P. Langhorst, Simultaneous changes of rhythmic organization in brainstem neurons, respiration, cardiovascular system and EEG between 0.05 Hz and 0.5 Hz, J. Auton. Nerv. Syst. **68**, 58 (1998).

[41] J. V. Ringwood and S. C. Malpas, Slow oscillations in blood pressure via a nonlinear feedback model, Am. J. Physiol. Regulatory. Integrative Comp. Physiol. **280**, R1105 (2000).

[42] A. M. Catai, C. M. Pastre, M. F. de Godoy, E. da Silva, A. C. M. Takahashia, and L. C. M. Vanderlei, Heart rate variability: Are you using it properly? Standardisation checklist of procedures, Braz. J. Phys. Ther. **24**, 91 (2020).

[43] P. Horowitz and W. Hill, *The Art of Electronics*, 3rd ed. (Cambridge University Press, Cambridge, UK, 2015).

[44] P. E. McSharry, G. D. Clifford, L. Tarassenko, and L. A. Smith, A dynamical model for generating synthetic electrocardiogram signals, IEEE Trans. Biomed. Eng. **50**, 289 (2003).

[45] T. Schreiber and A. Schmitz, Improved Surrogate Data for Nonlinearity Tests, Phys. Rev. Lett. **77**, 635 (1996).

[46] B. M. W. Illigens and C. H. Gibbons, Autonomic testing, methods and techniques, Handb. Clin. Neurol. **160**, 419 (2019).

[47] N. Montano, T. G. Ruscone, A. Porta, F. Lombardi, M. Pagani, and A. Malliani, Power spectrum analysis of heart rate variability to assess the changes in sympathovagal balance during graded orthostatic tilt, Circulation **90**, 1826 (1994).